Modelling Potential Rates of Natural Subsidence using Geological and PSI Ground Motion Data: An Experiment in Europe and Great Britain

Lee Jones[1], Luke Bateson[1], Andrew Hulbert[1] and Francesca Cigna[2*]

[1]British Geological Survey (BGS), Nicker Hill, Keyworth, Nottingham NG12 5GG, UK.

[2]Formerly at British Geological Survey (BGS), Nicker Hill, Keyworth, Nottingham NG12 5GG, UK.

Corresponding author: Lee Jones (ldjon@bgs.ac.uk)

*Now: Italian National Research Council, Piazzale Aldo Moro 7, Rome, Italy.

Key Points:

- Potential volume change (percentage) for all lithological units in Europe has been modelled for the natural processes of dissolution, compression and shrinkage.
- Volume change was then calibrated against measurements of subsidence for areas of known motion to give potential rates of motion (mm/yr).
- Derived relationship has been applied to 1:50 000 scale geology in Great Britian to give a national map of potential subsidence rates.

Abstract

Sixteen of the world's largest cities, with populations of over 10 Million, are located within 100 km of the coast (as are sixteen European cities, with populations of over 1 Million). The need to understand the contribution that the lowering of the ground surface, through natural geological phenomena, can make to estimates of relative sea level change is especially relevant to these lowland areas, which are usually the most geologically susceptible to subsidence. In this work, the methodology developed within the SubCoast EC-FP7 project was exploited to create a combined natural subsidence potential percentage change value for each lithology of the OneGeology dataset for Europe. Calibration of potential volume changes against ground motion statistics extracted from interpreted Persistent Scatterer Interferometry (PSI) and geohazard mapping datasets allowed for the deriva-tion of potential ground motion rates for the coastline of Europe. By utilising this subsidence po-tential methodology and combining it with the British Geological Survey (BGS) geology (superficial and bedrock) 1:50,000 scale dataset, a nation-wide dataset of potential natural subsidence rates was produced for Great Britain, providing information for all lithologies of the country. By incorporating the most current and up-to-date PSI data, the potential subsidence rates could be re-calculated, and a more detailed, calibrated polygon dataset could be created in the future. SubCoast was a collab-orative research project funded by the EU, the aim of which was to assess the combined impact of sea level rise and coastal subsidence as measured with satellite radar interferometry.

Plain Language Summary:

Of the thirty or so cities in the world with populations over 10 Million, sixteen of them are located within 100 km of the coast. These lowland cities are especially vulnerable to ground subsidence and sea level rise. This paper describes how the lithological component of these areas, in Europe and Great Britain, along with their potential to change in volume due to the natural processes of dissolution, compression and shrinkage can be modelled. This volume change is calibrated against subsidence measurements made from interpreted Persistent Scatterer Interferometry (PSI) to provide a relationship between potential ground motion rates and ground deformation.

1 Introduction

There is a need to understand the contribution that the lowering of the ground surface, through natural geological phenomena, can potentially make to estimates of sea level change. This is especially relevant to these coastal lowland areas, which tend to be highly populated and will experience the largest impact of sea level rise, but are also the most geologically susceptible to subsidence. With climate change forecasts in-dicating an increase in the frequency and intensity of winter storms and other adverse weather events these more susceptible, lower lying, coastal areas are more at risk of coastal flooding and inundation [1].

Coastal lowland areas are widely recognised as highly vulnerable to the impacts of climate change, particularly sea-level rise and changes in runoff, as well as being subject to stresses imposed by human modification of catchment and delta plain land use [2]. Utilisation of the coast increased dramatically during the 20th century, a trend that seems certain to continue through the 21st century. It has been estimated that 23% of the world's population lives both within 100 km distance of the coast and <100 m above sea level, and population densities in coastal regions are about three times high-er than the global average [3]. Sixty percent of the

world's 39 metropolises with a pop-ulation of over 5 million are located within 100 km of the coast, including 12 of the world's 16 cities with populations greater than 10 million [3].

Rates of relative sea-level rise can greatly exceed the global average in many heavily populated coastal lowland areas due to subsidence [4]. Natural subsidence due to compaction of sediment under its own weight is enhanced by sub-surface fluid withdrawals and drainage [5]. This increases the potential for inundation, coastal ero-sion, habitat disruption and salt water intrusion, especially for the most populated cit-ies on these coastal lowland areas. Aside from regional environmental effects of sub-sidence there are direct costs related to subsidence and soft soil conditions experienced in coastal lowland areas. Failure of constructions, infrastructure and water defence structures bring high maintenance costs with them and add up to substantial financial damages in these areas [4]. Typically, rates of subsidence vary over various spatial scales and depend strongly on local geological conditions and human activity.

The mainland of Great Britain is surrounded by over 17,500 km of coastline. It is a very diverse coastline both in terms of geology and geomorphology, ranging from the high chalk cliffs of Sussex to the flat expanses of The Wash and Morecambe Bay. The coast has been shaped by the continual forces of erosion from the wind, waves and tide and the characteristics and geological composition of the coastline will dictate the de-gree of its vulnerability to erosion, and to the effect of sea-level rise and coastal flood-ing [6.

Future UK climate predictions (UKCP18) predict that the threat of extreme weather events and sea-level rise, especially in coastal regions, means that more people are likely to be exposed to the effects of coastal erosion than ever [7]. Sea-level rise is pre-dicted to be in the order of 30 cm to 2 m by 2100, with the worst hit communities being the more densely populated areas of southern England [8]. These coastal areas, which are increasing in population, are more at risk because many of them are low lying, but also because the warmer climate means they are likely to experience more extreme weather and storms. As sea levels rise, so too will coastal erosion; this will lead to in-undation and changes in run-off in coastal lowland areas and in turn may lead to an increase in the amount of natural subsidence [6].

The British Geological Survey (BGS) previously carried out work under a Seventh Framework Programme (FP7) project, named SubCoast, which assessed and monitored subsidence hazards in coastal lowland areas around Europe. SubCoast was a collabo-rative project involving 12 partners, from seven European countries, aimed at devel-oping a pan-European GMES-downstream service for assessing, monitoring and fore-casting subsidence hazards in coastal lowland areas around Europe. The research was carried out in 2010 and completed in 2013 [4]. The core SubCoast product observes terrain height changes with time, which can be coupled with additional data (such as variations in sea-level) in order to improve our understanding of these coupled coastal dynamics. Creation of this Dynamic DEM, was undertaken for three pilot areas and required the input of a base DEM and measurements of ground deformation to alter the base DEM and add the dynamic element. However, ground motion data was not available for the entire European landmass, therefore to extend the SubCoast concept to the European scale it was necessary to consider alternative methods. The Potential Subsidence product was therefore devised, which shows the potential for European coastal zone areas to undergo subsidence due to the natural processes of compaction, dissolution and shrinkage of geological deposits. OneGeology (Europe) (1GE) [9] data was used to determine which geological deposits might undergo these processes, and to map them out across the European coastline. Measurements of ground motion from freely available EO data such as

ERS1/2, Envisat and Sentinel-1 satellite radar data were used to calibrate the geological data, thereby enabling rates of motion, in milli-metres, to be assigned to the European coastline.

This paper applies the lessons learnt during the SubCoast project and seeks to improve on the initial dataset by utilising the greater volume of data and degree of geological resolution available for Great Britain. The resultant dataset, described in this paper, provides theoretical maximum rates of natural subsidence for the entirety of Great Britain. Rates were derived by first considering the potential volume change a geolog-ical deposit could undergo given the optimum conditions. These potential volume changes were then calibrated using statistics extracted from satellite Interferometric Synthetic Aperture Radar (InSAR) observations of ground motion for interpreted nat-ural subsidence phenomena for 10 European towns.

Subsidence is the lowering or collapse of the ground and is possible where the ground material can be displaced into an underground void space [10]. It can be trig-gered by man-made disturbance, a change in drainage patterns, heavy rain or by water abstraction. Some fine soils collapse due to a restructuring that occurs when they are saturated for the first time; this is called hydrocompaction [10]. Rock salt, gypsum and limestone may be dissolved and removed naturally over time; solution is fastest in salt and slowest in limestone. Peat may contain up to 10 times its own weight in water and can shrink by 10-75% under load [10]. Clays have high porosity with deformable clay minerals [10]; loss of water and restructuring allows consolidation to occur, usually seen as subsidence of the surface and settlement of structures [11].

At the coast there are additional complications due to the interactive effects of erosion and landsliding, and the effects of extremely high-tides and storm surges. Subsidence has the potential to cause engineering problems such as damage to foundations, buildings and infrastructure. Subsidence events are associated with solution caves in karst, natural cavities in salt or gypsum, mining of coal and other rocks [12], or erosion of chalk (e.g. Birling Gap, East Sussex). Ground shrinkage can also occur in very porous, deformable rocks such as clays (e.g. Fairlight Cove, East Sussex), in fine-grained, low density soils such as windblown loess or rapidly deposited alluvial silts, in highly compressible soils such as peat, and in made ground or fill materials.

2 Input Datasets

Calibration of the potential subsidence model was accomplished using data from 10 towns (Table 1), these were chosen based on the availability of OneGeogy-Europe data, Persistent Scatterer Interferometry (PSI) data, geological geohazard interpreta-tions and the presence of the natural hazards considered in the development of the model. The required input datasets are described in more detail below.

2.1 Geological Data

2.1.1 OneGeology-Europe

OneGeology-Europe was a two-year project of the European Commission (eCon-tentPlus programme) between 2008 and 2010 to make a 1:1M scale harmonized sur-face geological map for Europe, attributes are Geologic unit, Age and Lithology [13]. This was completed or 26 European countries: Belgium, Czech Republic, Denmark, Es-tonia, Finland, France, Germany, Hungary, Ireland, Italy, Luxembourg, Netherlands, Norway,

Poland, Portugal, Slovakia, Slovenia, Sweden, Spain, United Kingdom (https://www.europe-geology.eu/onshore-geology/geological-map/onegeologyeurope/). The Lithology attributes are organised into five lithological fields, named 'urn_litho1' to 'urn_litho5', containing the lithological units used in the analysis. These fields are based on dominant lithologies (1) down to minor lithologies (5).

2.1.2 BGS Geology 1:50 000

The BGS Geology 1:50 000 scale dataset [14] is BGS's primary national geological reference dataset. It is compiled from individual digital tiles of data which were based on the traditional 'one-inch to one-mile' and 1:50,000 scale, paper geological maps; with each one typically covering an area of 20 x 29 km (12 x 18 miles). The geology is generalised from more detailed field-surveyed maps (typically between 1:10,000 and 1:25,000 scales) and it is the most extensive, moderately-detailed, geological interpre-tation available from BGS for onshore Great Britain.

The data are arranged into four geological themes: 1. Bedrock (e.g. rocks and de-posits laid down prior to 2.588 million years ago) 2. Superficial (e.g. deposits laid down during the Quaternary Period) 3. Mass Movement (e.g. areas of landslide) 4. Artificial (e.g. areas of artificially modified ground) And an additional component for: 5. Linear features (e.g faults) [15].

2.2 Ground Motion Datasets

Within the PanGeo project (section 2.3) PSI data (PSI is a remote sensing tech-nique that uses multiple SAR images acquired over the same area to measure and track slight changes on the Earth's surface. It is also known as Persistent Scatterer In-terferometric Synthetic Aperture Radar (PSInSAR)) were used to enable interpreta-tions of ground motions to deliver Ground Stablilty Layers for 52 European towns. These PSI data were also used to calibrate the subsidence potential methodology pre-sented in this paper. PSI is a well established technique to generate ground motion da-ta from the processing of long temporal stacks of satellite SAR imagery, using pointwise interferometric approaches [13]. Comparisons with other geodetic tech-niques show PSI achives accuracies in the order of a few mm/year, depending on sur-face characteristics of the processed area, quantity and quality of the input SAR im-agery, and quality of the PSI processing [16]. Table 1 provides information on the 14 PSI products for 10 different European cities used within the study.

Table 1 Input ground motion datasets for the 10 selected towns of Europe used for the calibration.

Town	Dataset(s)	Processing Method	PSI Provider	Value Adding Provider
Berlin	ERS-1/2 1992-2001	IPTA	Altamira Information	BGR
Warsaw	ERS-1/2 1992-2000	SPN	Altamira Information	PGI
Copenhagen	ERS-1/2 1992-2000	IPTA	GAMMA Remote Sensing AG	GEUS
Cork	ERS-1/2 1992-2000	IPTA	(FNPA)	GSI
Rome	ERS Desc 1992-2000	PSInSAR	TRE	ISPRA
Rome	Envisat Desc 2002-2005	PSInSAR	TRE	ISPRA

London	ERS+Envisat 1997 - 2005	IPTA	FNPA	BGS
London	ERS Asc 1992-2000	IPTA	FNPA	BGS
London	Envisat Desc 2002-2010	IPTA	FNPA	BGS
Hannover	ERS Desc 1992-2000	IPTA	FNPA	BGR
Hannover	ERS Asc 1992-2000	IPTA	FNPA	BGR
Nowy Sacz	ERS-1/2 1992-2000	SPN	Altamira Information	PGI
Maribor	Envisat Asc 2002-2009	IPTA	GAMMA Remote Sensing AG	GeoZS
Maribor	Envisat Desc 2002-2010	IPTA	GAMMA Remote Sensing AG	GeoZS
Maribor	ERS Desc 1992-2000	IPTA	GAMMA Remote Sensing AG	GeoZS
Prague	ERS Desc 1992-2005	IPTA	GAMMA Remote Sensing AG	CGS

2.3 Interpreted Ground Motion Layers

In order to derive statistics for areas of motion relating to known geohazards it is necessary to not only have the InSAR measurements of motion, but also to have an interpretation of such motions by a geologist: ideally this would consist of polygons outlining areas of known geohazards with corresponding InSAR measurement points within the polygon. PanGeo data provides just this.

PanGeo was a European Commission funded project under the Space Theme, Seventh Framework Programme (FP7-SPACE) which ran from 2011 to 2014 and was conceived to enable free and open access to geohazard information in support of Copernicus via the development of a validated Ground Stability Layer for 52 of the towns listed in the Copernicus Land Theme's Urban Atlas. Ground instability is mapped us-ing a variety of input datasets including existing geological data and PSI data. The PanGeo interpretation is not based on PSI data alone. Within PanGeo The integration and interpretation, plus a validation of key features observed, are made by the corre-sponding national geological survey for the towns concerned [13].

For each PanGeo town, areas of ground instability are indicated by attributed vector polygons held within the Ground Stability Layer. The polygon is supported by a detailed Geohazard Description document describing the interpretation of the geolog-ical reasons for the discovered motions. The Ground Stability Layer maps all the areas of a given town that are affected by ground instability, which can be caused by a number of natural and anthropogenic processes or phenomena, e.g. compressible ground, shrink-swell clays, ground dissolution, collapsible ground, landslides, soil creep, tectonic movements, underground construction works, fluid extraction or injec-tion, etc. The areas of mapped ground instability can fall into two categories:

1. Observed motion: includes all types of direct or indirect observation/measurement of ground motion.

2. Potential motion: includes all areas that the geologists, using the available geological and auxiliary data, have identified as having the potential for ground motion.

Examples of the PanGeo datasets include London where analysis of InSAR ground motion data and geological data allowed the identification of 25 geohazard polygons, covering a total of ~650 km2. These include not only natural processes such as

compac-tion of deposits on the River Thames flood plain and slope instability, but also anthro-pogenic instability due to groundwater management, recent engineering works, and the presence of made ground [17].

Whereas in Stoke-On-Trent the PanGeo process revealed 14 areas of natural and anthropogenic ground motion, with the dominant hazard relating to mine water level changes [18]. For Rome, 18 multipart polygons (covering ca. 600 km2) related to observed instabilities were outlined by ISPRA. Here ground movements could be detected through InSAR data or where landslides and sinkholes are known to have occurred. A further 13 multipart polygons (covering nearly 900 km2) concern areas where the potential occurrence of geohazards was inferred by combining geological and/or geothematic data (potential instabilities). The geohazards mapped in Rome are: landslides, collapsible grounds, compressible grounds, groundwater abstraction, mining, man-made ground, tectonic movements, and volcanic inflation/deflation [19].

3 Methodology

The derivation of calibrated potential rates of ground motion for Great Britain and Europe was a two-stage process:

1. Rates of potential volume changes were derived for all lithologies in the OneGeology Europe geological map.
2. These potential volume changes were calibrated against extracted statistical measures of motions extracted from interpreted InSAR dataset for 10 European towns.

3.1. Establishing potential volume change

In order to create a subsidence criterion for Europe, a European-wide geology dataset and a list of subsidence-prone deposits were required. OneGeology Europe proved ideal for this purpose. All hazard types associated with ground subsidence were considered; these being compressible ground [20], dissolution [21] and shrink–swell clays [22].
Each lithological unit in 1GE was considered against the hazard types and assigned a qualitative value. This was based on the units assumed susceptibility to the hazard as shown in Table 2. In particular:

- Compressible ground - values between 1 and 9 were assigned, with 1 being the most prone and 9 being the least prone to compression: peat has the highest value (1), as it is considered to be the most susceptible to this particular hazard, followed by organic rich sediment (2) down to sand (8), as it is considered to have a much lower susceptibility. All ‘non-susceptible’ lithologies have the lowest value (9).
- Ground dissolution - values between 1 and 8 were assigned, with 1 being the most prone an 8 being the least prone to dissolution: salt has the highest value (1), followed by anhydrite (2) down to dolomite (7). All ‘non-susceptible’ lithologies have the lowest value (8).
- Shrink–Swell – values between 1 and 12 were assigned, with 1 being the most prone and 12 being the least prone to Shrink–Swell: peat has the highest value (1), followed by clay (2) down to wacke (11). All ‘non-susceptible’ lithologies have the lowest value (12).

Following this, a semi-quantitative subsidence value was assigned to each of the lithological units, based on the expert elicitation of four highly respected geologists or

engineering geologists. This semi-quantitative value provides a measure of the relative volume change that each deposit might undergo; for example, Peat is the most compressible and therefore given a value of 100, whereas a Clay, relative to a peat, will compress 10 times less and is therefore given a value of 10. A fifth independent geologist validated the results and the values given in Table 2 were assigned, giving peat a value of 100 for both compressible and shrink–swell, and salt a value of 100 for dissolution. All 'non-susceptible' lithologies were assigned a value of 0 for all hazard types.

Table 2. Qualitative and semi-quantative valuation for OneGeology Europe lithological units, based on individual datasets.

Compressible	Qualitative	Semi-Quantitative	Dissolution	Qualitative	Semi-Quantitative	Shrink-Swell	Qualitative	Semi-Quantitative
Peat	1	100	Salt	1	100	Peat	1	100
Organic Rich	2	70	Anhydrite	2	70	Clay	2	90
Sapropel	3	50	Gypsum	2	70	Claystone	3	50
Ooze	4	10	Chalk	3	40	Diamicton	4	45
Clay	4	10	Limestone	5	30	Mudstone	5	40
Mud	6	8	Travertine	5	30	Diamictite	6	30
Silt	7	5	Dolomite	7	10	Lignite	6	30
Sand	8	1	Other	8	0	Ooze	8	20
Other	9	0				Mud	9	19
						Shale	10	5
						Wacke	11	1
						Other	12	0

In order the create an actual measure of potential volume change, termed a Potential Subsidence Potential (PSP), the following question was then asked of the ex-perts: "Based on a 1m thick 'fresh' deposit (of the lithology in question) subject to com-plete drying or full saturation, with fluid flow, under load, for ~10 years, the experts were asked to agree on:

- What percentage 'loss' will the deposit suffer?
- What percentage 'uplift' will occur in the deposit?"

This process resulted in the PSP values in Table 3, which shows the potential per-centage change expected for each lithological unit, for both subsidence (downward movement) and swelling (upward movement).

Table 3. Combined valuation (percentage change and occurrence in lithological fields).

Deposit	Subsidence			Swell		
	Litho_1/2	Litho_3/4	Litho_5	Litho_1/2	Litho_3/4	Litho_5

Peat	**90**	**60**	**30**	**10**	**7**	**3**
Organic Rich	**70**	**47**	**23**	**8**	**5**	**3**
Sapropel	**50**	**33**	**17**	**5**	**3**	**2**
Ooze	**50**	**33**	**17**	**2**	**1**	**1**
Clay	**33**	**22**	**11**	**40**	**27**	**13**
Mud	**19**	**13**	**6**	**20**	**13**	**7**
Claystone	**6**	**4**	**2**	**20**	**13**	**7**
Diamicton	**20**	**13**	**7**	**25**	**17**	**8**
Mudstone	**4**	**3**	**1**	**20**	**13**	**7**
Diamictite	**3**	**2**	**1**	**20**	**13**	**7**
Lignite	**25**	**17**	**8**	**5**	**3**	**2**
Silt	**5**	**3**	**2**	**0**	**0**	**0**
Sand	**2**	**1**	**1**	**0**	**0**	**0**
Shale	**5**	**3**	**2**	**10**	**7**	**3**
Wacke	**1**	**1**	**0**	**1**	**1**	**0**
Salt	**100**	**67**	**33**	**0**	**0**	**0**
Gypsum	**100**	**67**	**33**	**0**	**0**	**0**
Anhydrite	**100**	**67**	**33**	**60**	**40**	**20**
Other	**0**	**0**	**0**	**0**	**0**	**0**

The OneGeology Europe dataset consists of five lithological fields, named 'urn_litho1' to 'urn_litho5', containing the lithological units used in the analysis. These fields are based on dominant lithologies (urn_litho1) down to minor lithologies (urn_litho5). Using these fields, if a susceptible deposit occurs in urn_litho1 or urn_litho2 the PSP value assigned to it remains the same, if a deposit occurs in urn_litho3 or urn_litho4 the PSP value is reduced by one-third (33%), and if a deposit occurs in urn_litho5 the PSP value is reduced by two-thirds (66%). For example, peat has a PSP value of 90, for subsidence, if it occurs in urn_litho1 or 2, 60 if it occurs in urn_litho3 or 4, and 30 if it occurs in urn-litho5. Similarly, salt has a PSP value of 100, for subsidence, if it occurs in urn_litho1 or 2, 67 if it occurs in urn_litho3 or 4, and 33 if it occurs in urn-litho5. These values were calculated for both subsidence and swelling (Table 3). The lithological units with both 'subsidence' and 'swell' values equalling 0 (zero) were discarded. The polygons for the remaining units were taken from OneGe-ology Europe and merged into a shapefile, in GIS, where two new fields were created. These were named 'SubComb' representing the PSP value for subsidence and 'Swell-Comb' representing the PSP value for swelling.

Since OneGeology Europe covers all European countries and there were slight inconsistencies it was necessary to remove certain units from the lithological fields (sedimentary material; sediment; sedimentary rock; chemical sedimentary material; clastic sediment; biogenic sediment; clastic sedimentary rock; organic rich sedimentary rock; evaporite; organic rich sediment). Where these were removed the remaining lithological units were moved-up the urn_litho order to take the place of the deleted lithology in the higher 'urn_litho'.

The methodology was designed to assign the highest subsidence, or swell, value possi-ble, and a subsidence potential map (Figure 1) was produced for the whole Europe (limited to countries where the OneGeology Europe layer was available; see Section 2.1).

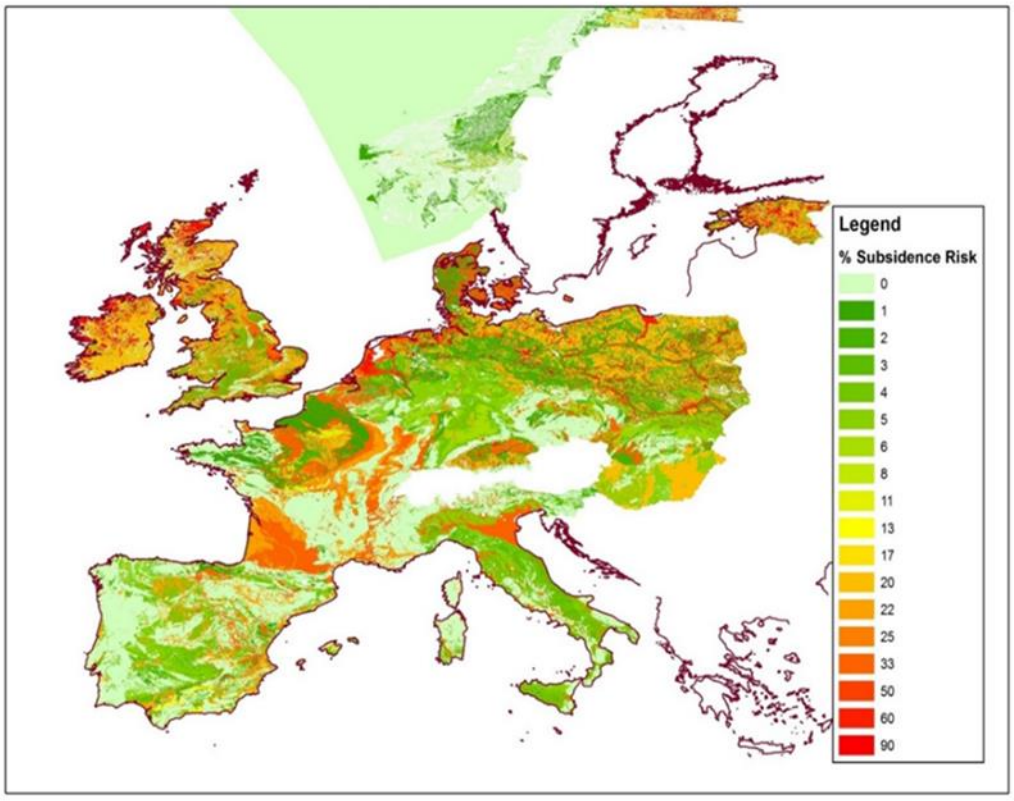

Figure 1. Potential subsidence of Europe.

3.2. Persistent Scatterer Interferometry (PSI) calibration of potential percentage change values

The aim of the calibration was to assign a rate of ground motion (mm/year) to each Potential Subsidence Potential (PSP) value and apply it to the whole 1GE dataset for the coastal areas of Europe to create a map of potential rates of coastal subsidence.

To calibrate the PSP predictions, satellite PSI data provided independent estimates of ground motion observed at the selected 10 calibration cities (see Section 2.2). Areas within the 1GE polygons that were susceptible to natural subsidence and for which the PSI data showed measurable ground motion were selected based on the interpreted geohazard mapping datasets produced by the EC-FP7 PanGeo project (see Section 2.3). These identify which areas are moving and what the reason for the motion is, thus allowing the focusing of the analysis only on PSI statistics from relevant geological hazards (i.e. natural processes of ground compaction, dissolution and collapsibility).

For each calibration town, statistics on observed ground motion rates were extracted from the PSI datasets for the 1GE polygons mapped within the town and affected by the natural geohazards defined above. Statistics for the 10 towns were then combined together to establish the Potential Subsidence Rate (PSR) for each PSP percentage change *j*.

As a first attempt for a potential calibration statistic, the simple average of the observed ground motion velocities (V_i) at each town *i* for the PSP value *j*:

$$PSR_j = \frac{1}{n}\sum_{i=1}^{n} V_i \qquad (1)$$

where *n* is the number of towns among the 10 considered for the calibration, that provided a statistic for the PSP_j value.

Resulting PSR_j simple average values computed for all PSP percentages are given in the second column of Table 4. On the whole these are as expected, i.e. the deposits for which the predicted subsidence was lower (lower PSP value) typically show a smaller PSR. However, this approach does not consider the size of the geohazard mapping polygon for which the PSI statistics were extracted, or how many points contributed to the average ground motion statistics.

Table 4. Derived statistics of ground motion velocities for each subsidence potential percentage.

PSP [%]	PSR Simple Average [mm/year]	PSR Weighted Average [mm/year]	PSR Weighted Average – 2*SDV [mm/year]
0	-0.788	-1.032	-4.360
1	-0.380	-0.380	-2.286
2	-1.394	-0.692	-2.769
3	-1.759	-1.117	-2.907
4	-2.228	-1.598	-4.130
5	-1.276	-1.475	-4.727
6	-1.170	-1.170	-1.170
20	-1.009	-0.954	-2.117
22	-0.498	-0.426	-2.096
33	-1.633	-0.860	-3.635
47	-1.504	-1.979	-5.812
60	-1.183	-1.066	-2.634
90	-2.655	-3.331	-8.551

Notation: PSP, Potential Subsidence Potential; PSR, Potential Subsidence Rate; SDV, standard deviation.

To account for the number of PSI points used to derive the average annual velocity for the different PSP values from the 10 calibration towns, a weighting was applied to give preference to statistics derived from a higher number of points. This assumes that more points lead to a statistically more robust average and that when more points are used it should help mitigate any outliers (i.e. value not directly correlated with the lead natural geohazard process mapped within the polygon).

The number of PSI points (N_i) available for each town to compute the statistics for a certain PSP value was used to weight the corresponding V_i statistic. The PSR_j for each PSP value j was therefore computed as:

$$PSR_j = \sum_{i=1}^{n} (V_i * N_i) \Big/ \sum_{i=1}^{n} N_i \qquad (2)$$

Resulting weighted average PSR values for the various PSP percentages are shown in column 3 of Table 4. While the trend generally shows a moderate correlation (R2=0.47) between PSP and PSR observations (Figure 2) – with higher motion velocities observed for greater PSP values – there seem to be significant variability, especially at the lower PSP, and the maximum subsidence rates seem not in line with those expected from experience of PSI data interpretation [23].

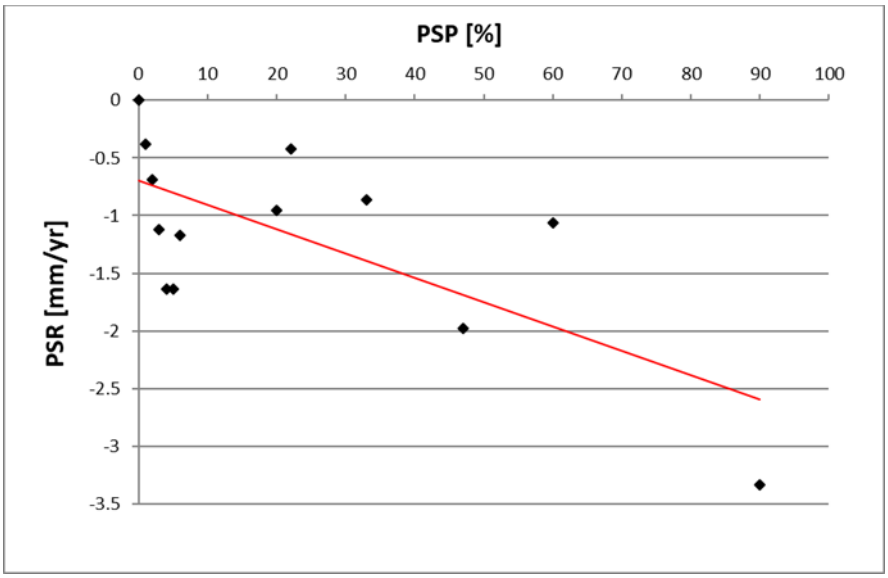

Figure 2. Weighted average of observed PSI annual velocity for the different PSP values.

The combined statistic V_i-2*σ_i (where σ_i is the velocity standard deviation) was tested as a further calibration approach to attribute subsidence rates to each PSP value, with the aim to identify a more realistic maximum rate value which a deposit could subside by. This is, indeed, generally not provided by the average of observed motions (i.e. V_i) as this might include points that are stable, or are undergoing motion which is not related to the subsidence mechanisms that are not considered here (e.g., anthropogenic geohazards). Similarly, the maximum negative ground motion velocity values cannot be used, as these are not necessarily representative of the typical subsidence rate that a deposit might undergo – as they could be due to other factors and motion mechanisms.

By exploiting the two-sigma empirical rule for normally distributed data (i.e. nearly 95.45% of the values lie within two standard deviations of the mean), the subtraction of 2*σ_i from V_i allowed us to filter out ~2.275% of the velocity data close to the negative edge of the distribution. This was considered a derived statistics providing a more suitable representation for the PSR that a certain PSP values could result in.

The adjusted PSR_j for each PSP value j was therefore computed as:

$$PSR_j = \sum_{i=1}^{n} [(V_i - 2\sigma_i) * N_i] \Big/ \sum_{i=1}^{n} N_i \qquad (3)$$

The results of this weighted statistics for the various PSP values are shown in the fourth column of Table 4.

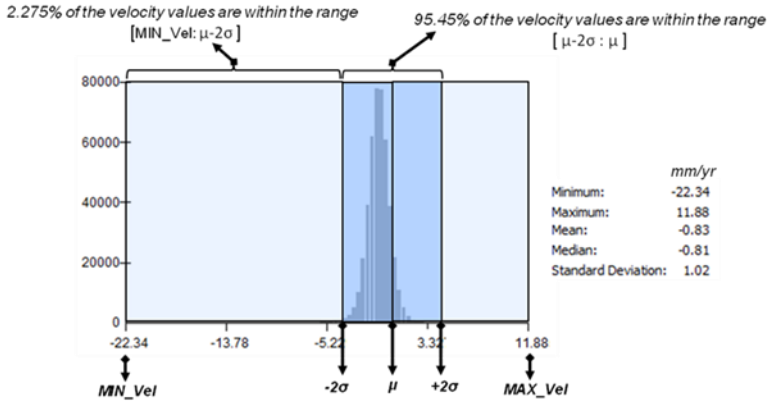

Figure 3. Example of PSI velocity data distribution for 1GE urn_litho1=silt.

As the extracted calibration values only exist for certain PSP values (i.e. those coincident with PanGeo interpretations and PSI data availability; see Sections 2.2 and 2.3), in order to extend the calibration to other PSP values a linear regression was applied to extract the trend on available observations, and calculate the missing PSP values. Unexpectedly high annual velocities values were observed from the PSI statistics at low PSP (Table 4). These are thought to be artificially high due to the inconsistency between the mapping scale of OneGeology Europe data (i.e. nominally, 1:1 million; see Section 2.1), the interpreted PanGeo geohazard mapping products (i.e. nominally 1:10,000; see Section 2.3) and input PSI data (typically, hundreds of targets per square km). Ground motion statistics for PSP values between 0 and 5% (which are clearly affected by such an inconsistency) were therefore excluded from the calibration plot used to derive the subsidence rates (Figure 4).

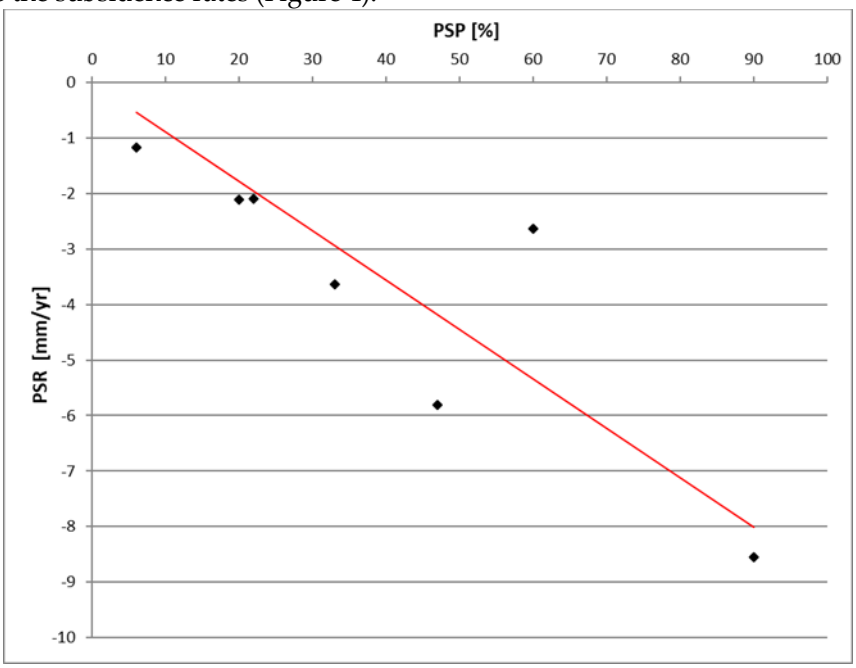

Figure 4. Calibration plot: weighted average velocities vs SubComp predictions (PSP vs PSR).

The equation for the linear trend observed in Figure 4 was then used to derive the expected PSR for any given PSP, by fixing the intercept at 0 (i.e. a PSP value of 0% will have a PSR of 0 mm/year):

$$PSR_j = -0.089 * PSP_j \quad (4)$$

This means that for each increase of 1% in PSP, we consider an increase of 0.089 mm/year in the corresponding predicted ground motion velocity. The full set of predicted PSR values for each PSP based on the above linear function is shown in Table 5.

Table 5. Calibrated PSR for each PSP value.

PSP [%]	PSR [mm/year]
0	0.000
1	-0.089
2	-0.178
3	-0.267
4	-0.356

5	-0.445
6	-0.534
8	-0.712
11	-0.979
13	-1.157
17	-1.513
20	-1.780
22	-1.958
25	-2.225
33	-2.937
47	-4.183
50	-4.450
60	-5.340
67	-5.963
70	-6.230
90	-8.010
100	-8.900

3.3. Application to Great Britain at the 1:50,000 Scale

Application to Great Britain requires the lithological codes from the BGS Geology dataset to be matched to the OneGeology Europe lithological codes, and hence matched to the PSP values. BGS Geology 1:50,000 scale [13] was identified as the most appropriate dataset to use due to it being the most detailed dataset with complete Great Britain coverage. Rates of natural subsidence are usually small and therefore take place in the surface geology. It was therefore necessary to consider all geological codes from the bedrock and the superficial datasets.

The BGS Rock Classification Scheme (RCS) is a system for classifying and naming geological materials as they appear at the scale of a single exposure, hand specimen, or thin section. In the first instance RCS_D (RCS Description) values for the UK 1:50,000 superficial geology were mapped to the PSP values (0-100%), based on the potential subsidence percentage (urn_litho_1/2 values in Table 3). In the case where multiple lithologies are identified in the RCS_D, the worst case (i.e. lithology most prone to subsidence) was used. The potential subsidence values were then matched to the calibrated PSR as derived from Table 5.

It is necessary to account for the thickness of superficial deposits when assigning a PSP. If the superficial is thicker than 5 m then it is only the superficial which is considered to subside. However, when there are between 1 and 5 m of superficial the combined contribution of the bedrock and superficial was considered (following the procedure detailed in [14]). This was done via use of the superficial thickness model and used the conditions set out in Table 6.

Table 6. PSP values selection for Great Britain based on thickness of superficial deposits.

Superficial thickness [m]	PSP to use
0 (no superficial cover)	Use bedrock PSP
1-3	Use maximum PSP of the superficial or bedrock
3-5	If bedrock PSP is 25% or greater, then use maximum PSP of superficial or bedrock. If bedrock PSP is less than 25% then use superficial PSP
> 5	Use superficial PSP

405 The 'deposits' in OneGeology Europe (Table 3) are descriptive of the geological deposits this
406 can therefore be linked to the RCS_D attribute in the BGS geology dataset. Linking the PSP from
407 OneGeology Europe to BGS Geology was therefore straightforward. Once the RCS_D had an
408 associated PSP attribute the PSR attribute could be linked too (Figure 5 – Print-screen of table).

RCS	RCS_D	PSP	PSR mm/yr
B	BOULDERS	0	0
BCSU	BLOCKS, CLAST-SUPPORTED [UNDIFFERENTIATED]	0	0
CATUFA	TUFA, CALCAREOUS	0	0
DIATOM	DIATOMITE	0	0
NONE	NO SUPERFICIAL	0	0
REGOL	REGOLITH	0	0
RFA	ROCK FRAGMENTS, ANGULAR, UNDIFFERENTIATED SOURCE ROCK	0	0
SDSH	SEDIMENT, SHELL (SHELLS)	0	0
SED	SEDIMENT	0	0
UKNOWN	UNKNOWN	0	0
V	GRAVEL	0	0
WATR	WATER AT SURFACE	0	0
XBGR	BOULDERS, GRANITE	0	0
XBVSZ	BOULDERS, GRAVEL, SAND AND SILT	0	0
XVFLY	GRAVEL, FLINTY	0	0
XVLSR	GRAVEL, LIMESTONE-RICH	0	0
LMST	LIMESTONE	1	-0.079
S	SAND	2	-0.157
SV	SAND, GRAVELLY	2	-0.157
VS	GRAVEL, SANDY	2	-0.157
XSV	SAND AND GRAVEL	2	-0.157
XSVB	SAND, GRAVEL AND BOULDERS	2	-0.157
SZ	SAND, SILTY	5	-0.393
SZV	SAND, SILTY, GRAVELLY	5	-0.393
VZ	GRAVEL, SILTY	5	-0.393
XSVZ	SAND, GRAVEL AND SILT	5	-0.393
XSZ	SAND AND SILT	5	-0.393
XVSZ	GRAVEL, SAND AND SILT	5	-0.393
XZSV	SILT, SAND AND GRAVEL	5	-0.393
XZV	SILT AND GRAVEL	5	-0.393
Z	SILT	5	-0.393
ZS	SILT, SANDY	5	-0.393
MUD	MUD	19	-1.4915
XMS	MUD, SANDY	19	-1.4915
XVSM	GRAVEL, SAND AND MUD	19	-1.4915
DMRC	DIAMICTON WITH CHALK RAFTS	20	-1.57
DMTN	DIAMICTON	20	-1.57
XDCSV	DIAMICTON, CLAY, SAND AND GRAVEL	20	-1.57
XDSV	DIAMICTON, SAND AND GRAVEL	20	-1.57
XDV	DIAMICTON AND GRAVEL	20	-1.57
XDVSZ	DIAMICTON, GRAVEL, SAND AND SILT	20	-1.57

409

C	CLAY	33	-2.591
CLSH	CLAY, SHELL	33	-2.591
CS	CLAY, SANDY	33	-2.591
CSV	CLAY, SANDY, GRAVELLY	33	-2.591
CSVL	CLAY, SANDY, GRAVELLY, COBBLY	33	-2.591
CSVZ	CLAY, SANDY, GRAVELLY, SILTY	33	-2.591
CV	CLAY, GRAVELLY	33	-2.591
CVS	CLAY, GRAVELLY, SANDY	33	-2.591
CZ	CLAY, SILTY	33	-2.591
CZPS	CLAY, SILTY, PEATY, SANDY	33	-2.591
CZS	CLAY, SILTY, SANDY	33	-2.591
CZV	CLAY, SILTY, GRAVELLY	33	-2.591
SC	SAND, CLAYEY	33	-2.591
SCV	SAND, CLAYEY, GRAVELLY	33	-2.591
VC	GRAVEL, CLAYEY	33	-2.591
VSCZ	GRAVEL, SANDY, CLAYEY, SILTY	33	-2.591
XCS	CLAY AND SAND	33	-2.591
XCSV	CLAY, SAND AND GRAVEL	33	-2.591
XCV	CLAY AND GRAVEL	33	-2.591
XCZ	CLAY AND SILT	33	-2.591
XCZS	CLAY, SILT AND SAND	33	-2.591
XCZSP	CLAY, SILT, SAND AND PEAT	33	-2.591
XCZSV	CLAY, SILT, SAND AND GRAVEL	33	-2.591
XSC	SAND AND CLAY	33	-2.591
XSCB	SAND, CLAY AND BOULDERS	33	-2.591
XSVCZ	SAND, GRAVEL, CLAY AND SILT	33	-2.591
XSWCV	SAND WITH CLAY AND GRAVEL	33	-2.591
XSZC	SAND, SILT AND CLAY	33	-2.591
XVSZC	GRAVEL, SAND, SILT AND CLAY	33	-2.591
XZC	SILT AND CLAY	33	-2.591
XZCS	SILT, CLAY AND SAND	33	-2.591
P	PEAT	90	-7.065
XCPZ	CLAY, PEAT AND SILT	90	-7.065
XCZP	CLAY, SILT AND PEAT	90	-7.065
XPMOMC	PEAT, ORGANIC MUD AND CALCAREOUS MUD	90	-7.065
XPZ	PEAT AND SILT [EITHER DOMINANT LOCALLY]	90	-7.065

410

411 **Figure 5.** BGS Superficial geology coded up for PSP and PSR values.

4 Results and Discussion

Figure 6 shows the satellite calibrated subsidence potential map for the coastal (5 m contour) areas of Europe. As expected we see highest potential rates of subsidence (6-8mm/yr) in the deltaic areas such as the Wash in the UK, to Po Delta in Italy and the Rhine Meuse delta of the Netherlands. These are all associated with compressible geo-logical deposits of Peat and Alluvium. Whilst not necessarily coastal lowlands we also observe high rates of potential subsidence (6-9mm/yr) in the bog peats of Northern Scotland and Ireland which happen to be near to the coastline. The low-lying sandy Aquitaine western coast of France shows more moderate rates of subsidence (~2mm/yr) relating to the subordinate clay present in a largely sandy superficial deposit.

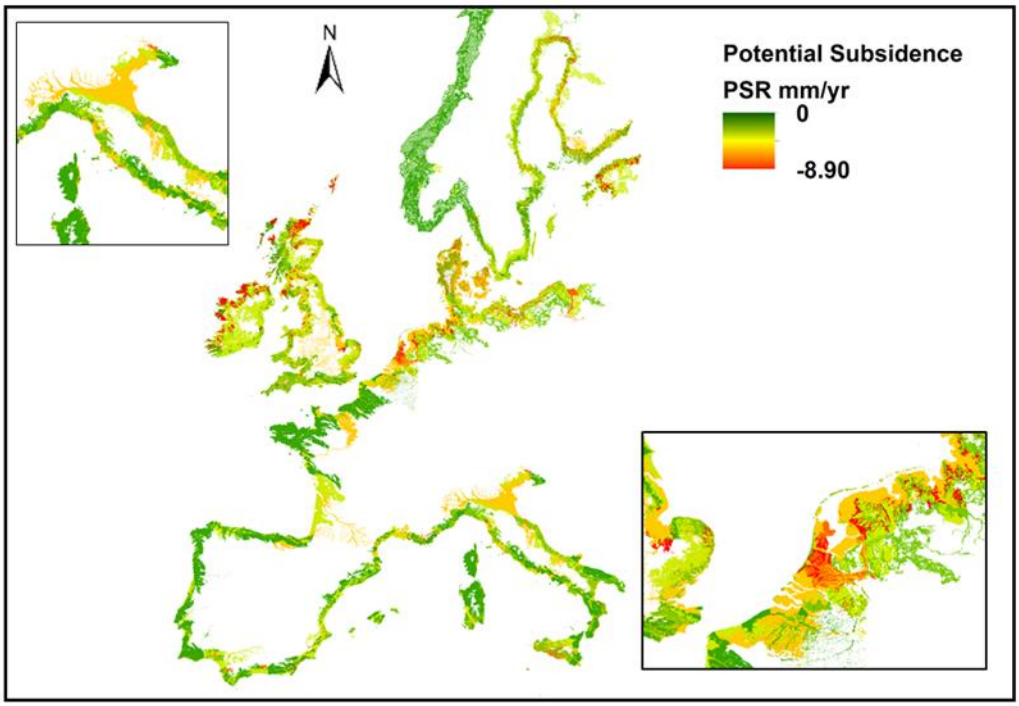

Figure 6. Satellite calibrated subsidence potential map for the coastline area (5 m contour) of Europe. Insets show detail for the Netherlands and Northern Italy.

Figure 7 shows the satellite calibrated subsidence potential map for the whole landmass of Great Britain.

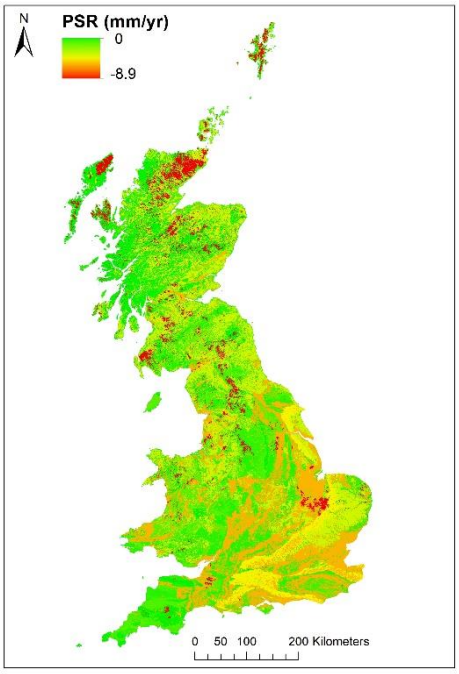

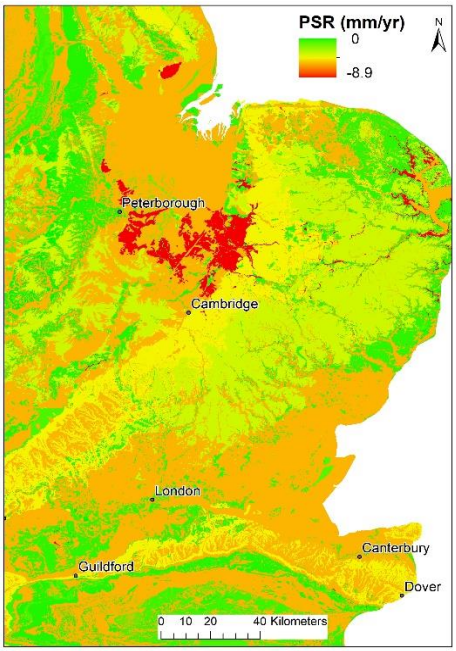

Figure 7. a. Potential Subsidence Rates for Great Britain. **b.** Potential Subsidence rates for the east and south east of Great Britain highlighting the Wash area and London.

As expected the majority of the hard rock areas of the UK are stable with potential rates of motion of zero mm/yr as show in green in Figure 7a. Therefore, the north west of the UK appears more stable than the south east. The exception area areas of peat of the flow country of north west Scotland, the Isle of Sky, the Cairngorms and Pennines of northern England. These are typically upland peat and have potential motions rates of 7-8mm/yr, which aligns well with the 7.2mm/yr that Alshammari et al [24] found using the ISBAS InSAR technique and applying it to Sentinel 1 data for the same area.

The south east of the UK is geologically younger and therefore more susceptible to the natural subsidence resulting from processes such as compression and shrinkage. In particular the mudstones and clays of the London basin and Weald are susceptible to shrinkage.

Estuarine areas, with thick unconsolidated deposits show medium potential rates of subsidence. For example, the Thames valley shows a potential subsidence rate of ap-proximately -2.5mm/yr, detailed interpretations of InSAR data for London [17] show this to be accurate for the subsidence related to compressible ground. In fact Aldiss et al [25] interpret a domain of subsidence along the Thames from GNSS corrected InSAR measurements which has an overall average velocity of -2mm/yr, they attribute this motion to compression of Holocene deposits.

The same is true for the Wash area (Figure 7b) to the west of Norfolk where rates of motion of approximately 3mm/yr are predicted, these relate to the higher clay con-tent in the recent alluvial sediments. To the south of the Wash are higher potential rates of 7-8mm/yr associated with the potentially highly compressible peat deposits. The Chalk outcrop of the UK is clearly visible with potential subsidence rates of ap-proximately -2mm/yr relating to the potential process of dissolution.

Advantages and disadvantages to the approach:

One of the main advantages to modelling expected rates of natural subsidence and calibrating them with InSAR measurements is that it gives a basis to recognise such subsidence within InSAR ground motions datasets. The rates we have derived can be used to train machine learning algorithms to identify natural subsidence in large InSAR datasets. For example, the European Ground Motion Service (EGMS [26]) con-tains over 6 million measurement points for the UK alone, manual analysis of so many points and their time series is not possible, therefore having training datasets which characterise the motion characteristics for subsidence phenomena is essential to better use these new data.

Advantage: this technique provides a quick means to identify, from the geological information, which areas are susceptible to ground motions and provide an indication of the likely rates of such motion. This can be used by decision makers, planning au-thorities etc to understand the potential rates of motion for a given area. The technique derived, in independent of the input geological data and can therefore be applied to any geological dataset which includes the lithological description.

Advantages and disadvantages of the methods and data used:

For the European case we had to use the OneGeology Europe dataset as this is all that is available, this is only 1:250 000 scale and has therefore been generalised so will not provide as

493 detailed an understanding as would be possible with higher resolution data. However, saying this
494 it was a collaboration of many countries, unprecedented around the world. In the UK we have
495 access to the 1:50 000 scale geological data. Due to the generalisation process the OneGeology
496 Europe dataset has up to 5 levels of data relating to the abundance of a geological unit. Level one
497 the most abundant, level 5 the least. The method has accounted for these but it is possible that a
498 highly susceptible material in one of the lower levels will be under represented according to its
499 propensity to cause motion and therefore potential motion rates might be lower than actual.

500 The calibration was based on available calibration data from the FP7 PanGeo project.
501 Within the method it was essential that we could extract rates of motion for areas that we knew
502 were moving due to a certain subsidence mechanism. We therefore needed interpreted data, this
503 was only available for a small number of sites. It would have been ideal to have a much larger
504 number of interpreted sites available to us. Also, although the interpretations had been completed
505 according to a standardised interpre-tation approach, they were spread across Europe and
506 therefor represent different geo-logical formations. Although a clay in the UK and a clay in
507 Germany are undergoing shrinkage the mechanisms of shrinkage, and hence the rate are not
508 exactly the same, especially as the two clays will probably also be made up of different
509 mineralogies.

510 Developed using ERS and Envisat data, this was necessary as these were the da-taset
511 which underwent the standardised interpretation in the PanGeo project, however they also
512 represent an older InSAR data product compared to what might be generated now with Sentinel -
513 1 data. The earlier InSAR data have a less frequent revisit time meaning the sampling of the
514 ground motion measurements are not as great and in some cases may be subject to unwrapping
515 issues which could potentially introduce er-ror.

516 ***Application prospects:***

517 Can be applied to any geology data worldwide to give an indication of potential rates of
518 natural subsidence

519 Can be used as a training dataset for machine learning to automatically interpret the huge
520 InSAR datasets we are starting to see.

521 Can be used as part of a national coastal geology dataset (such as GeoCoast) to better
522 inform stakeholders on their exposure to hazards and processes at the coasts: one of the most
523 dynamic environments.

524 **5 Conclusions**

525 Sixteen of the world's largest cities, with populations of over 10 Million, are lo-cated
526 within 100 km of the coast. (as are sixteen European cities, with populations of over 1 Million).
527 The need to understand the contribution that the lowering of the ground surface, through natural
528 geological phenomena, can make to estimates of sea level change is especially relevant to these
529 lowland areas, which are usually the most geologically susceptible to subsidence [27].

530 The methodology developed within the SubCoast FP7 project allowed for:

1. Creation of a combined Subsidence value for each OneGeology Europe derived lithologies, by establishing the Volume Change Potential of each lithological unit (Figure 1).

2. Derivation of PSI calibrated potential ground motion for the European coastline (5m contour), by calibrating these potential volume changes against statistical measures of motions extracted from interpreted InSAR datasets for 10 European towns (Figure 6).

3. Production of a detailed nation-wide map of potential natural subsidence for Great Britain, providing information for all lithologies of the country, by utilising the subsidence potential methodology and combining it with the BGS Geology (Super-ficial and Bedrock) 1:50,000 scale dataset.

These maps not only tell us where subsidence is likely to take place but also the po-tential rate of such subsidence, this is important to people who have an interest in the land; they may wish to build upon it and therefore need to understand what potential ground motion they need to mitigate against in the design of the construction. They might also be responsible for existing buildings or infrastructure and therefore need an understanding of the rates of motions to understand how those might affect the asset. Making this data consistently available over the entire country wide scales allows for consistent profiling of nation-wide asset portfolios.

An understanding of todays expected rates of motion, which are driven under the existing climatic conditions, is an essential starting point for any future forecast of po-tential rates of motion under different climatic conditions. Shrink-Swell processes are driven by the removal or addition of water, long hot dry summers, such as those expe-rienced in 2018 and 2022, lead to increased subsidence. We are able to model different climatic outcomes for different future climatic scenarios, an understanding of pre-sent-day rates of shrink-swell motion is a starting point to understand rates under the different future climatic outcomes.

Potential rates of subsidence linked to natural processes are essential to interpret, identify and understand such processes in a measurement dataset; datasets such as those presented in this paper are therefore an invaluable tool to enable the interpreta-tion of InSAR datasets. This becomes especially important when we consider that SAR data is becoming increasingly freely available and therefore derived datasets, such as InSAR, are also becoming more common. These freely available InSAR resources, such as the European Ground Motions Service (EGMS: https:/egms.land.copernicus.eu/), represent large volumes of data covering wide spatial areas. Although valuable as a dataset the real value in such resource is the information they contain, extracting the information requires a concerted data integration and interpretation effort. Ideally such an effort will be automated, the starting point for any automated InSAR inter-pretation routine needs to be a detailed understanding of the rates associated with a process. This dataset provides exactly this for natural subsidence processes and there-fore forms an essential learning dataset for future automatic interpretation routines.

By incorporating the most current and up-to-date PSI data, the potential subsid-ence rates could be re-calculated and a more detailed, calibrated polygon dataset could be created in the future.

Acknowledgments

This paper is published with permission of the director of the British Geological Survey. The authors would also like to acknowledge Geologists at the British Geological Survey who took part in the expert elicitation process used to establish the semi-quantitative value assigned to each of the lithological units: David Entwistle, Peter Hobbs, Don Aldiss, Kevin Northmore and Anthony Cooper.

The authors declare no conflict of interest.

This research received no external funding.

References

1. Wong, P.P., I.J. Losada, J.-P. Gattuso, J. Hinkel, A. Khattabi, K.L. McInnes, Y. Saito, and A. Sallenger, 2014: Coastal systems and low-lying areas. In: Climate Change 2014. Impacts,Adaptation, and Vulnerability. Part A: Global and Sectoral Aspects. Contribution of Working Group II to the Fifth Assessment Report of the Intergovernmental Panel on Climate Change [Field, C.B., V.R. Barros, D.J. Dokken, K.J. Mach, M.D. Mastrandrea, T.E. Bilir, M. Chatterjee, K.L. Ebi, Y.O. Estrada, R.C. Genova, B. Girma, E.S. Kissel, A.N. Levy, S. MacCracken, P.R. Mastrandrea, and L.L.White (eds.)]. Cambridge University Press, Cambridge, United Kingdom and New York, NY, USA, pp. 361-409.

2. Nicholls, R.J., P.P. Wong, V.R. Burkett, J.O. Codignotto, J.E. Hay, R.F. McLean, S. Ragoonaden and C.D. Woodroffe, 2007. Coastal systems and low-lying areas. Climate Change 2007: Impacts, Adaptation and Vulnerability. Contribution of Working Group II to the Fourth Assessment Report of the Intergovernmental Panel on Climate Change, M.L. Parry, O.F. Canziani, J.P. Palutikof, P.J. van der Linden and C.E. Hanson, Eds., Cambridge University Press, Cambridge, UK, 315-356.
3. The Ocean Conference, 2017. *Factsheet* [online]. Available at: https://www.un.org/sustainabledevelopment/wp-content/uploads/2017/05/Ocean-fact-sheet-package.pdf [Accessed December 2021].
4. Bateson, L., Evans, H. and Jordan, C. 2011. GMES-Service for Assessing and Monitoring Subsidence Hazards in Coastal Lowland Areas around Europe. *European Commission Research Executive Agency*. Seventh Framework Programme Theme 9 – Space.
5. Candela, T. and Koster, K. 2022. The many faces of anthropogenic subsidence. *Science*, 376: 1381-1382. https://doi.org/10.1126/science.abn3676
6. Oppenheimer, M., B.C. Glavovic , J. Hinkel, R. van de Wal, A.K. Magnan, A. Abd-Elgawad, R. Cai, M. Cifuentes-Jara, R.M. DeConto, T. Ghosh, J. Hay, F. Isla, B. Marzeion, B. Meyssignac, and Z. Sebesvari, 2019. Sea Level Rise and Implications for Low-Lying Islands, Coasts and Communities. In: IPCC Special Report on the Ocean and Cryosphere in a Changing Climate [H.-O. Pörtner, D.C. Roberts, V. Masson-Delmotte, P. Zhai, M. Tignor, E. Poloczanska, K. Mintenbeck, A. Alegría, M. Nicolai, A. Okem, J. Petzold, B. Rama, N.M. Weyer (eds.)].In Press.
7. Met Office. 2019. UK Climate Projections: Headline Findings. Met Office, Hadley Centre, Exeter.
8. BBC. 2020. *Vulnerable Coastlines* [online]. Available at: https://www.bbc.co.uk/bitesize/guides/z3qhxfr/revision/1 [Accessed December, 2021].
9. BGS, 2020. *OneGeology [online]*. Available at http://www.onegeology.org/home.html. [Accessed December 2021].
10. Waltham, T., 2009. Foundations of Engineering Geology. *Spon Press*. Oxfordshire, UK.
11. Fokker, P.A., Gunnink, J.L., Koster, K. and de Lange, G. 2019. Disentangling and Parameterizing Shallow Sources of Subsidence: Application to a Reclaimed Coastal Area, Flevoland, the Netherlands. *JGR Earth Surface*. https://doi.org/10.1029/2018JF004975

12. Declercq, P-Y., Dusar, M., Pirard, E., Verbeurgt, J., Choopani, A. and Devleeschouwe, X. Post 2023. Mining Ground Deformations Transition Related to Coal Mines Closure in the Campine Coal Basin, Belgium, Evidenced by Three Decades of MT-InSAR Data. *Remote Sensing*. Vol.15(3), DOI:10.3390/rs15030725
13. Laxton, J,. Serrano, J-J. amd Tellez-Arenas, A. 2010. Geological applications using geospatial standards – an example from OneGeology-Europe and GeoSciML, International Journal of Digital Earth, 3:sup1, 31-49, DOI: 10.1080/17538941003636909.
14. BGS. 2020. BGS Geology 50K [online]. Available at: https://www.bgs.ac.uk/products/digitalmaps/DiGMapGB_50.html. [Accessed December 2021].
15. Armstrong, R. A., Daley, D. L., Lawley, R., Myers, A. H, and Smith, A. 2016. User Guide for the BGS Geology: 50k dataset (V8). British Geological Survey Open Report, OR/16/46. 25pp
16. Crosetto, M., Monserrat, O., Iglesias, R. and Crippa, B., 2010. *Persistent Scatterer Interferometry: Potential, Limits and Initial C- and X-band Comparison*. Photogrammetric Engineering and Remote Sensing, *76*(9): 1061–1069.
17. Cigna, F., Jordan, H., Bateson, L. *et al.* 2015. Natural and Anthropogenic Geohazards in Greater London Observed from Geological and ERS-1/2 and ENVISAT Persistent Scatterers Ground Motion Data: Results from the EC FP7-SPACE PanGeo Project. *Pure Appl. Geophys.* **172,** 2965–2995 (2015). https://doi.org/10.1007/s00024-014-0927-3
18. Jordan H., Cigna F., Bateson L. 2017. Identifying natural and anthropogenically-induced geohazards from satellite ground motion and geospatial data:Stoke-on-Trent, UK. (2017) International Journal of Applied Earth Observation and Geoinformation, 63 , pp. 90-103.
19. Comerci, V., Vittori, E., Cipolloni, C. *et al.* 2015. Geohazards Monitoring in *Roma* from InSAR and In Situ Data: Outcomes of the PanGeo Project. *Pure Appl. Geophys.* **172,** 2997–3028 (2015). https://doi.org/10.1007/s00024-015-1066-1
20. Jones, L., Diaz Doce, D., Lee, K. and Entwisle, D. 2014. GeoSure Version 7 Methodology: Compressible Ground. *British Geological Survey Internal Report*. IR/14/015
21. Farrant, A., Cooper, A. and Diaz Doce, D. 2014. GeoSure Version 7 Methodology: Soluble Rocks (Dissolution). *British Geological Survey Internal Report*. IR/14/012
22. Diaz Doce, D., Jones, L. and Lee, K. 2014. GeoSure Version 7 Methodology: Shrink-Swell. *British Geological Survey Internal Report*. IR/14/017
23. Bateson, Luke; Cuevas, Maria; Crosetto, Michele; Cigna, Francesca; Schijf, Marlies; Evans, Hannah. 2012 PANGEO : enabling access to geological information in support of GMES : deliverable 3.5 production manual. Version 1. *European Commission*, 104pp. OR/12/053
24. Alshammari, L.; Large, D.J.; Boyd, D.S.; Sowter, A.; Anderson, R.; Andersen, R.; Marsh, S. Long-Term Peatland Condition Assessment via Surface Motion Monitoring Using the ISBAS DInSAR Technique over the Flow Country, Scotland. *Remote Sens.* **2018**, *10*, 1103. https://doi.org/10.3390/rs10071103
25. Aldiss, D., Burke, H., Chacksfield, B., Bingley, R., Teferle, N., Williams, S., Blackman, D. and Burren, R. 2014. Nigel Press,. Geological interpretation of current subsidence and uplift in the London area, UK, as shown by high precision satellite-based surveying, Proceedings of the Geologists' Association, Volume 125, Issue 1, 2014, Pages 1-13, ISSN 0016-7878, https://doi.org/10.1016/j.pgeola.2013.07.003.
26. European Ground Motion Service (EGMS) Costantini, M., Minati, F., Trillo, F., Ferretti, A., Novali, F., Passera, E., Dehls, J., Larsen, Y., Marinkovic, P., Eineder, M., Brcic, R., Siegmund, R., Kotzerke, P., Probeck, M., Kenyeres, A., Proietti, S., Solari, L. and Andersen, H.S. 2021. *IEEE International Geoscience and Remote Sensing Symposium IGARSS*, Brussels, Belgium, 2021, pp. 3293-3296, doi: 10.1109/IGARSS47720.2021.9553562
27. Gerardo Herrera-García, Pablo Ezquerro, Roberto Tomás, Marta Béjar-Pizarro, Juan López-Vinielles, Mauro Rossi, Rosa M. Mateos, Dora Carreón-Freyre, John Lambert, Pietro Teatini, Enrique

663 Cabral-Cano, Gilles Erkens, Devin Galloway, Wei-Chia Hung, Najeebullah Kakar, Michelle
664 Sneed, Luigi Tosi, Hanmei Wang and Shujun Y. 2021. Mapping the global threat of land subsidence.
665 Science. Vol 371, Issue 6524, pages 34-36, DOI: 10.1126/science.abb8549